

Stochastic transitions of attractors in associative memory models with correlated noise

Masaki KAWAMURA¹ * and Masato OKADA²³

¹*Graduate School of Science and Engineering, Yamaguchi University*

Yoshida 1677-1, Yamaguchi-shi, Yamaguchi, 753-8512 Japan

²*Department of Complexity Science and Engineering, Graduate School of Frontier Sciences, The University of Tokyo, 5-1-5 Kashiwanoha, Kashiwa-shi, Chiba, 277-8562 Japan,*

³*Computational Neuroscience Research Group, RIKEN Brain Science Institute, 2-1 Hirosawa, Wako, Saitama, 351-0198 Japan.*

We investigate dynamics of recurrent neural networks with correlated noise to analyze the noise's effect. The mechanism of correlated firing has been analyzed in various models, but its functional roles have not been discussed in sufficient detail. Aoyagi and Aoki have shown that the state transition of a network is invoked by synchronous spikes. We introduce two types of noise to each neuron: thermal independent noise and correlated noise. Due to the effects of correlated noise, the correlation between neural inputs cannot be ignored, so the behavior of the network has sample dependence. We discuss two types of associative memory models: one with auto- and weak cross-correlation connections and one with hierarchically correlated patterns. The former is similar in structure to Aoyagi and Aoki's model. We show that stochastic transition can be presented by correlated rather than thermal noise. In the latter, we show stochastic transition from a memory state to a mixture state using correlated noise. To analyze the stochastic transitions, we derive a macroscopic dynamic description as a recurrence relation form of a probability density function when the correlated noise exists. Computer simulations agree with theoretical results.

KEYWORDS: common external input, correlated noise, associative memory, stochastic transition, macroscopic dynamic description

1. Introduction

In the activities of nerve cells, synfire chains, i.e., synchronous firings of neurons, can often be observed.¹ To analyze the mechanism of synchronous firings, conditions for propagating them between layers have been investigated in layered neural networks.^{2,3} Common synaptic inputs to neurons have been introduced in layered neural networks, and correlated firings of neurons have been investigated on a theoretical level.⁴ We have also analyzed common synaptic inputs in recurrent neural networks, i.e., a sequential associative memory model,⁵ and succeeded in deriving a macroscopic dynamic description as a recurrence relation form of a probability density function. On another front, investigating the functional roles of syn-

*E-mail address: kawamura@sci.yamaguchi-u.ac.jp

chronous firings has become important. Associative memory models, which store patterns as attractors, are used to explain these roles. Aoyagi and Aoki^{6,7} have investigated a model with auto- and weak cross-correlation connections and showed that a transition between attractors cannot be invoked by thermal independent noise but can be by synchronous spikes. In general, when using thermal independent noise, the state leaves an attractor for another one. However, Aoyagi and Aoki's model can make the state transit to the next attractor by synchronous spikes, i.e., external inputs.

In this paper, we consider two types of associative memory models with *a common external input*. The common external input affects all neurons equally and therefore invokes correlated firings of neurons. To analyze dynamic behavior theoretically, we assume that common external input obeys Gaussian distribution and acts like correlated, not independent, noises.

The first model consists of an autoassociative memory model^{8,9} and a weakly connected sequential associative memory model,^{10–13} as well as Aoyagi and Aoki's model.^{6,7} Associative processing requires functions of both autoassociative memory, which retrieves a memory pattern from an ambiguous initial state, and sequential associative memory, which retrieves memory patterns episodically.¹⁴ This model contains these functions. To switch from autoassociative to sequential associative, we introduce external inputs. One input is an independent (thermal) noise and the other is a correlated noise (a common external input). The synchronous spikes in Aoyagi and Aoki's model can be considered correlated noises in our model since they invoke correlated firings. We examine the effectiveness of the independent and correlated noises, and demonstrate that stochastic transition can be presented by correlated, but not independent, noise, as shown in Figure 1(a).

The second model we consider is an associative memory model that stores hierarchically correlated patterns.^{15–19} In this case, both the memory states and their mixture states are attractors.²⁰ We demonstrate that a stochastic transition from a memory to a mixture state can be invoked by the correlated rather than the independent noise, as shown in Figure 1(b).

Almost all existing models have been analyzed by applying independent units or neurons at the thermodynamic limit. Since we introduce correlated noises in these models, the sum of the inputs to the neurons are correlated. Therefore, the firings of the neurons are also correlated. With an infinite number of neurons, there is no thermodynamic limit and sample dependence appears.^{4,21} Theoretical approaches that address sample dependence are described by probability density functions (PDF) for macroscopic states or order parameters.^{5,22} Yamana and Okada²² have introduced uniform common synaptic inputs that depend on preneurons to a layered associative memory model and derived the PDF. Kawamura *et al.*⁵ have introduced common synaptic inputs to recurrent neural networks and derived a macroscopic dynamic description as a recurrence relation form of the PDF. The common synaptic inputs that depend

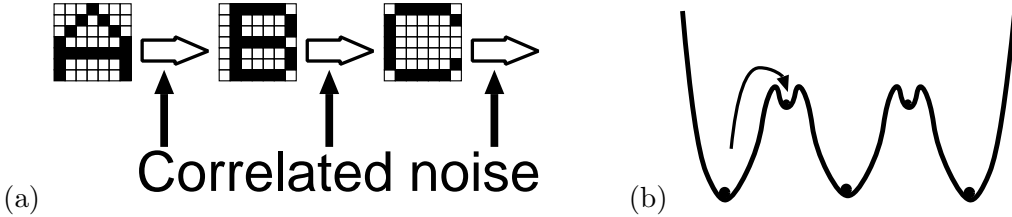


Fig. 1. Schematic illustrations of (a) stochastic transition by correlated noise in an associative memory model with auto- and weak cross-correlation connections, and (b) transition from memory to mixture state in one with hierarchically correlated patterns.

on preneurons were analyzed in these previous papers.^{23–25} In this paper, we analyze external rather than synaptic inputs and derive a macroscopic dynamic description as a recurrence relation form of the PDF.

This paper is organized as follows. In the next section, we examine the first model, i.e., the model with auto- and weak cross-correlation connections. Theoretical results and those obtained using computer simulations are given. In §3, we examine the second model, i.e., the model that stores hierarchically correlated patterns. The final section is devoted to conclusion.

2. Autoassociative and sequential associative memory model

2.1 Model

We consider the associative memory model consisting of N units or neurons and introduce two types of external input: independent external input ζ_i^t , which affects each neuron independently, and common external input η^t , which affects all neurons mutually. The state of the neurons takes $x_i^t = \pm 1$ and is updated synchronously by

$$x_i^{t+1} = F \left(\sum_{j \neq i}^N J_{ij} x_j^t + \zeta_i^t + \eta^t \right), \quad (1)$$

where the output function is $F(h) = \text{sgn}(h)$, and J_{ij} is a synaptic connection from the j th to the i th neuron. Here, the synapse has both auto- and weak cross-correlation connections and stores p random patterns $\xi^\mu = (\xi_1^\mu, \dots, \xi_N^\mu)^T$, $\mu = 1, 2, \dots, p$. The element of the patterns takes ± 1 with

$$\text{Prob} [\xi_i^\mu = \pm 1] = \frac{1}{2}. \quad (2)$$

The synaptic connection J_{ij} is given by

$$J_{ij} = \frac{1}{N} \sum_{\mu=1}^p \xi_i^\mu \xi_j^\mu + \frac{\varepsilon}{N} \sum_{\mu=1}^p \xi_i^{\mu+1} \xi_j^\mu, \quad (3)$$

where $\xi_i^{p+1} = \xi_i^1$ and ε denotes a connecting parameter. Under normal conditions, that is, without noise, the model behaves as an autoassociative memory model, since the connecting parameter is very weak $\varepsilon \ll 1$.

We define the overlap by the direction cosine between the state of neurons, \mathbf{x}^t , at time t and the memory pattern $\boldsymbol{\xi}^\mu$,

$$m_t^\mu = \frac{1}{N} \sum_{i=1}^N \xi_i^\mu x_i^t. \quad (4)$$

From (3) and (4), the state of the neurons, x_i^{t+1} , becomes

$$x_i^{t+1} = F \left(\sum_{\mu=1}^p \xi_i^\mu m_t^\mu + \varepsilon \sum_{\mu=1}^p \xi_i^{\mu+1} m_t^\mu + \zeta_i^t + \eta^t \right) \quad (5)$$

$$= F \left(\sum_{\mu=1}^p (\xi_i^\mu + \varepsilon \xi_i^{\mu+1}) m_t^\mu + \zeta_i^t + \eta^t \right). \quad (6)$$

The initial state \mathbf{x}^0 is determined according to the probability distribution

$$\text{Prob}[x_i^0 = \pm 1] = \frac{1 \pm m_0 \xi_i^1}{2}. \quad (7)$$

Therefore, the overlap between the pattern $\boldsymbol{\xi}^1$ and the initial state \mathbf{x}^0 is m_0 .

2.2 Theory

Let us derive the macroscopic description of the model with the external inputs. In order to simplify the argument, we assume that the number of memory patterns, p , is finite, especially when $p = 3$. The independent external input ζ_i^t is time independent and independent of each neuron x_i^t . In addition, we assume ζ_i^t obeys the Gaussian distribution with $\mathcal{N}(0, \Delta^2)$. The correlated external input η^t is time independent, and is assumed to obey the Gaussian distribution with $\mathcal{N}(0, \delta^2)$. These external inputs are called independent noise and correlated noise.

2.2.1 Without correlated noise ($\eta^t = 0$)

First, we discuss the case without correlated noise, $\eta^t = 0$. Since there is only independent noise, when $N \rightarrow \infty$, the overlap $m_{t+1}^\mu, \mu = 1, 2, 3$ becomes

$$m_{t+1}^\mu = \frac{1}{N} \sum_{i=1}^N \xi_i^\mu F \left(\sum_{\nu=1}^3 (\xi_i^\nu + \varepsilon \xi_i^{\nu+1}) m_t^\nu + \zeta_i^t \right), \quad (8)$$

$$= \left\langle \int D_z \xi^\mu F \left(\sum_{\nu=1}^3 (\xi^\nu + \varepsilon \xi^{\nu+1}) m_t^\nu + \Delta z \right) \right\rangle_\xi, \quad (9)$$

$$= \left\langle \xi^\mu \text{erf} \left(\frac{\sum_{\nu=1}^3 (\xi^\nu + \varepsilon \xi^{\nu+1}) m_t^\nu}{\sqrt{2} \Delta} \right) \right\rangle_\xi, \quad (10)$$

where $D_z = \frac{dz}{\sqrt{2\pi}} \exp\left(-\frac{z^2}{2}\right)$ and $\langle \cdot \rangle_\xi$ denotes the average over the memory pattern $\boldsymbol{\xi}^\mu$. The function $\text{erf}(u)$ is defined as

$$\text{erf}(u) = \frac{2}{\sqrt{\pi}} \int_0^x dt \exp(-t^2). \quad (11)$$

In this case, we find that the macroscopic parameter m_t^μ is deterministically given.

2.2.2 With correlated noise ($\eta^t \neq 0$)

In the case with correlated noise, the states of the neurons are correlated, because the common external input is introduced into all neurons mutually. Therefore, sample dependence must be taken into account. We derive a macroscopic dynamic description as a recurrence relation form of a probability density function (PDF).

The correlated noise distributes $\eta^t \sim \mathcal{N}(0, \delta^2)$. When η^t is known at given time t and $N \rightarrow \infty$, then $m_{t+1}^\mu, \mu = 1, 2, 3$ can be given as a function of m_t^1, m_t^2, m_t^3 , and η^t ,

$$m_{t+1}^\mu(m_t^1, m_t^2, m_t^3, \eta^t) = \left\langle \int Dz \xi^\mu F \left(\sum_{\nu=1}^3 (\xi^\nu + \varepsilon \xi^{\nu+1}) m_t^\nu + \Delta z + \eta^t \right) \right\rangle_\xi, \quad (12)$$

$$= \left\langle \xi^\mu \text{erf} \left(\frac{\sum_{\nu=1}^3 (\xi^\nu + \varepsilon \xi^{\nu+1}) m_t^\nu + \eta^t}{\sqrt{2}\Delta} \right) \right\rangle_\xi. \quad (13)$$

Using this equation, the dynamic behavior of the model for various δ can be analyzed. When $\delta = 0$, the model corresponds to the existing associative memory models and behaves deterministically. However, when $\delta > 0$, the values of m_t^1 , m_t^2 , and m_t^3 are distributed. This distribution can be described as the PDF, $p(m_t^1, m_t^2, m_t^3, \eta^t)$. Since η^t is independent of m_t^1 , m_t^2 , and m_t^3 , $p(m_t^1, m_t^2, m_t^3, \eta^t)$ can be divided into two PDFs:

$$p(m_t^1, m_t^2, m_t^3, \eta^t) = p(m_t^1, m_t^2, m_t^3) p(\eta^t). \quad (14)$$

Therefore, the PDF can be given by

$$\begin{aligned} p(m_{t+1}^1, m_{t+1}^2, m_{t+1}^3) &= \int \prod_{\nu=1}^3 dm_t^\nu d\eta^t p(m_t^1, m_t^2, m_t^3) p(\eta^t) \\ &\times \prod_{\nu=1}^3 \delta(m_{t+1}^\nu - m_{t+1}^\nu(m_t^1, m_t^2, m_t^3, \eta^t)), \end{aligned} \quad (15)$$

where $\delta(\cdot)$ denotes the Dirac delta function defined as

$$\delta(u) = \begin{cases} \infty, & u = 0 \\ 0, & u \neq 0 \end{cases}. \quad (16)$$

The PDF $p(\eta^t)$ is given by

$$p(\eta^t) = \frac{1}{\sqrt{2\pi}\delta} \exp\left(-\frac{(\eta^t)^2}{2\delta^2}\right). \quad (17)$$

Then, we combine this with the integral of η^t and obtain equations

$$p(m_{t+1}^1, m_{t+1}^2, m_{t+1}^3) = \int \prod_{\nu=1}^3 dm_t^\nu p(m_t^1, m_t^2, m_t^3) K(m_{t+1}^\nu; m_t^\nu), \quad (18)$$

$$K(m_{t+1}^\nu; m_t^\nu) = \int d\eta^t p(\eta^t) \prod_{\nu=1}^3 \delta(m_{t+1}^\nu - m_{t+1}^\nu(m_t^1, m_t^2, m_t^3, \eta^t)). \quad (19)$$

We can also calculate (19) directly, but we evaluate it using the Monte Carlo method in the following section.

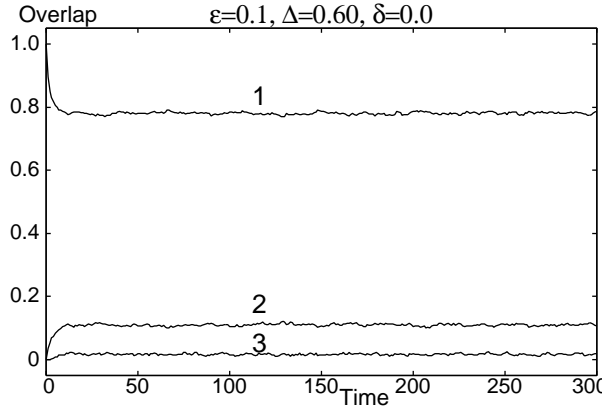


Fig. 2. Time evolutions of overlaps m_t^1 , m_t^2 , and m_t^3 using a computer simulation in the case without correlated noise, where $\varepsilon = 0.1$ and $\Delta = 0.6$.

2.3 Results

The first case is without correlated noise η^t , that is, $\delta = 0.0$. Figure 2 shows time evolutions of the overlaps m_t^1 , m_t^2 , and m_t^3 using a computer simulation, where the standard deviation (SD) of the independent noise ζ_i^t is $\Delta = 0.6$. The connecting parameter is $\varepsilon = 0.1$. Numbers in Figure 2 denote indexes of the memory patterns. We find that no transition occurs even if large independent noise is induced. The model acts like the autoassociative memory model through to the end.

Next, we consider the case with correlated noise η^t . Figure 3 shows time evolutions of the overlaps m_t^1 , m_t^2 , and m_t^3 using computer simulations ($N = 60,000$), where SDs of the independent and correlated noises are $\Delta = 0.1$ and $\delta = 0.37$. Figure 3(a) and (b) show results of the different trials. Therefore, we can verify that sample dependence exists and that the correlated noise invokes stochastic transition. The model acts like the sequential associative memory model. In the case of smaller correlated noise, transition probability to the next attractor is much smaller. However, in the case of larger noise, the state becomes much noisier, and we cannot identify what pattern is retrieved. Therefore, the appropriately sized correlated noise should be introduced in the model.

Let us consider sample dependence. Figure 4 shows the time evolution of the overlaps m_t^1 , m_t^2 , and m_t^3 . The number of neurons is $N = 60,000$. Each figure shows 20 samples. The initial overlap is $m_0 = 1.0$. When sample dependence appears, we need to consider the distribution, not the overlaps, of the samples. From the joint probability density function $p(m_t^1, m_t^2, m_t^3)$ in (18), we evaluate the marginal probability density function of m_t^μ , $\mu = 1, 2, 3$,

$$p(m_t^\mu) = \int \prod_{\nu \neq \mu} dm_t^\nu p(m_t^1, m_t^2, m_t^3). \quad (20)$$

Figure 5 shows the marginal PDF of the overlaps, $p(m_t^1)$, $p(m_t^2)$, $p(m_t^3)$ at time $t = 10$, 50 in Figure 4. Abscissas denote overlap m_t^μ , and ordinates denote marginal PDF $p(m_t^\mu)$

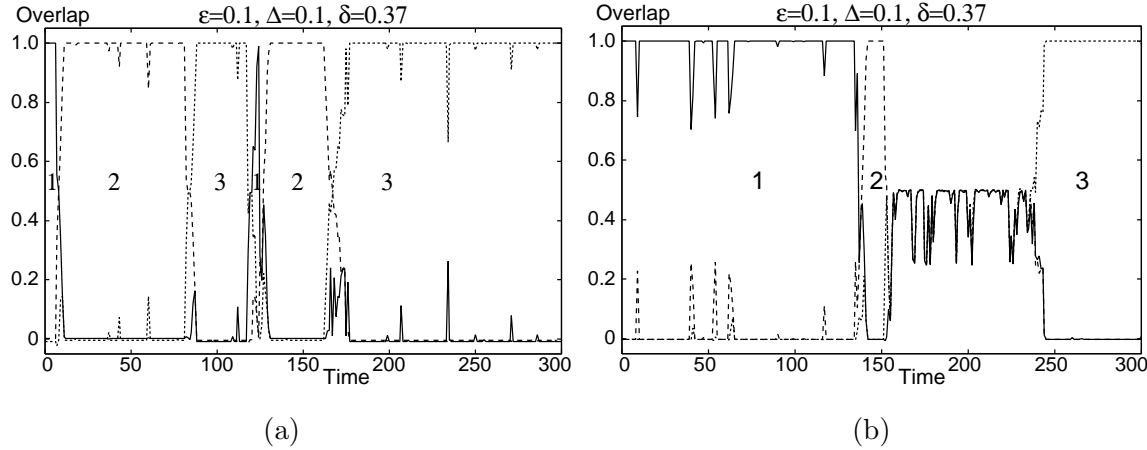


Fig. 3. Time evolutions of overlaps m_t^1, m_t^2 , and m_t^3 using computer simulations in the case with correlated noise, where $\varepsilon = 0.1, \Delta = 0.6$, and $\delta = 0.37$. (a) and (b) show results of different trials.

on a logarithmic scale. Boxes denote histograms of 1,000 samples, which are obtained using computer simulations ($N = 60,000$), and lines denote theoretical results. The theoretical results agree with the computer simulations. The state at time $t = 10$ distributes around the memory state ξ^1 , since the overlap m_{10}^1 takes the maximum in $m_{10}^1 = 1.0$. The state at time $t = 50$ also distributes around that of ξ^2 . As time passes, these PDFs approach a uniform distribution asymptotically.

We discussed the case when a common external input obeys the Gaussian distribution. We can, however, choose alternative common external input. The state transition seems to be caused by certain common external input. We empirically found a particular common external input. Figure 6 shows the state transition using the following external input:

$$\eta^t = \begin{cases} 1 & , t \bmod 10 = 0 \\ 0.5 & , t \bmod 10 = 1 \\ 0 & , \text{otherwise} \end{cases} \quad (21)$$

Thick vertical lines denote the particular common external input η^t . For instance, if a sequence of the external inputs is $\eta^{10} = 1$ and $\eta^{11} = 0.5$, then the state transition $\xi^2 \rightarrow \xi^3$ can occur the next time. When this is repeated, the memory patterns are retrieved sequentially. In this manner, the common external input to the neurons can control the transitions.

3. Associative memory model with hierarchically correlated patterns

3.1 Model

Now we discuss the associative memory model with hierarchically correlated patterns. Parent patterns $\xi_i^\mu, \mu = 1, 2, \dots, p$ are generated at random, and then child patterns $\xi_i^{\mu,\nu}, \nu = 1, 2, \dots, k$ are generated from the parent patterns ξ_i^μ with similarity r , that is, they are given

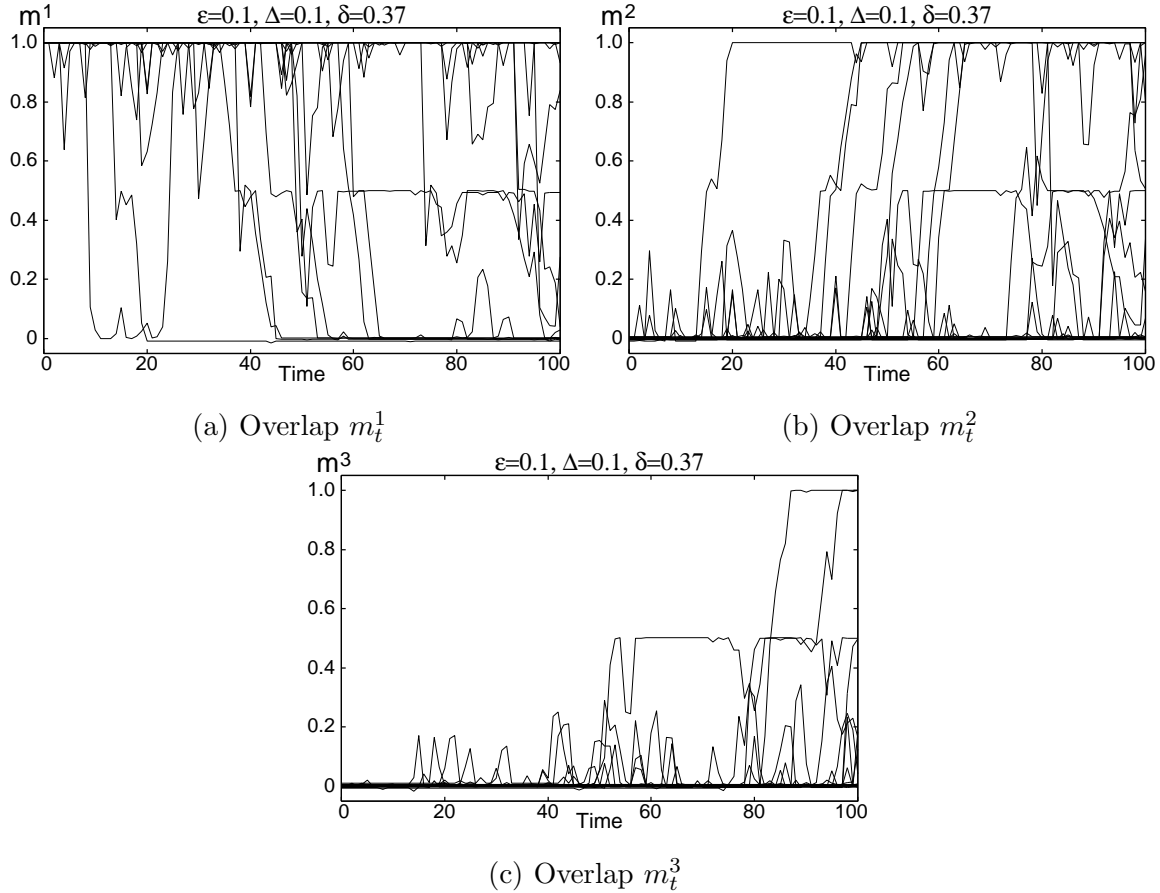


Fig. 4. 20 samples of overlaps m_t^1 , m_t^2 , and m_t^3 starting from $m_0 = 1.0$ using computer simulations, where $\varepsilon = 0.1$, $\Delta = 0.1$, and $\delta = 0.37$. (a) shows results of overlap m_t^1 , (b) for m_t^2 , and (c) for m_t^3 .

by

$$P[\xi_i^\mu = \pm 1] = \frac{1}{2}, \quad (22)$$

$$P[\xi_i^{\mu,\nu} = \pm 1] = \frac{1 + r\xi_i^\mu}{2}. \quad (23)$$

The child patterns having different parents are independent of each other, but those having the same parent are correlated. In the limit of $N \rightarrow \infty$, the correlations become

$$E[\xi_i^{\mu,\nu} \xi_i^{\tilde{\mu},\tilde{\nu}}] = 0, \quad \mu \neq \tilde{\mu}, \quad (24)$$

$$E[\xi_i^{\mu,\nu} \xi_i^{\mu,\tilde{\nu}}] = \begin{cases} 1, & \nu = \tilde{\nu} \\ r^2, & \nu \neq \tilde{\nu} \end{cases}. \quad (25)$$

The synaptic connection stores only the child patterns $\xi_i^{\mu,\nu}$ and is given by

$$J_{ij} = \frac{1}{N} \sum_{\mu=1}^p \sum_{\nu=1}^k \xi_i^{\mu,\nu} \xi_j^{\mu,\nu}. \quad (26)$$

Mixture states of the child patterns also become attractors even if only the child patterns are stored.²⁰

To make the argument simple, we assume that the numbers of the parent and child patterns, p and k , are finite, especially when $p = 1$ and $k = 3$. When the similarity is $r = 0$, that is, the child patterns are independent of each other, the mixture states become unstable faster than the memory states with an increase in temperature.²⁶ When $r > 0$, the mixture states become stabler. We define the overlap by the direction cosine between the state of neurons, \mathbf{x}^t , at time t and the child pattern $\boldsymbol{\xi}^{1,\mu}$,

$$m_t^\mu = \frac{1}{N} \sum_{i=1}^N \xi_i^{1,\mu} x_i^t. \quad (27)$$

From Equations (1), (26), and (27), the state x_i^{t+1} becomes

$$x_i^{t+1} = F \left(\sum_{\kappa=1}^3 \xi_i^{1,\kappa} m_t^\kappa + \zeta_i^t + \eta^t \right). \quad (28)$$

3.2 Theory

As in the case of the previous model, let us derive the PDF of this model. In the case without correlated noise η^t , when $N \rightarrow \infty$, the overlap m_{t+1}^μ can be

$$m_{t+1}^\mu = \left\langle \int D_z \xi^{1,\mu} F \left(\sum_{\kappa=1}^3 \xi^{1,\kappa} m_t^\kappa + \Delta z \right) \right\rangle_\xi, \quad (29)$$

$$= \left\langle \xi^{1,\mu} \text{erf} \left(\frac{\sum_{\kappa=1}^3 \xi^{1,\kappa} m_t^\kappa}{\sqrt{2}\Delta} \right) \right\rangle_\xi, \quad (30)$$

where $\langle \cdot \rangle_\xi$ denotes the average over not only the child patterns $\boldsymbol{\xi}^{1,\kappa}$, but also their parent pattern $\boldsymbol{\xi}^1$.

In the case that η^t would be known at given time t and $N \rightarrow \infty$, then m_{t+1}^μ could be given as the function of m_t^1 , m_t^2 , m_t^3 , and η^t ,

$$m_{t+1}^\mu(m_t^1, m_t^2, m_t^3, \eta^t) = \left\langle \int D_z \xi^{1,\mu} F \left(\sum_{\kappa=1}^3 \xi^{1,\kappa} m_t^\kappa + \Delta z + \eta^t \right) \right\rangle_\xi, \quad (31)$$

$$= \left\langle \xi^{1,\mu} \text{erf} \left(\frac{\sum_{\kappa=1}^3 \xi^{1,\kappa} m_t^\kappa + \eta^t}{\sqrt{2}\Delta} \right) \right\rangle_\xi. \quad (32)$$

Substituting Equations (18) and (19), we can obtain the recurrence relation form of the PDF for this model.

3.3 Function of External Noise

3.3.1 Without correlated noise ($\eta^t = 0$)

We show dynamic behaviors without correlated noise η^t . To verify retrieval of a memory state of a child pattern, we evaluated retrieval processes for various initial overlaps. Figure 7 shows the retrieval processes for the initial overlaps $m_0 = 0.1, 0.2, \dots, 1.0$. The abscissas and

ordinates denote the overlaps m_t^1 and m_t^2 . Solid and broken lines denote results obtained using computer simulations ($N = 60,000$) and Equation (10). When $\Delta \leq 0.3$, the state is attracted to the attractor of $\xi^{1,1}$ for a significantly large initial overlap. When $\Delta = 0.4$ or has a small initial overlap, the state goes to mixture state, not the memory state. We find that independent noise cannot invoke a transition to the mixture state once the state is attracted to the memory state.

3.3.2 With correlated noise ($\eta^t \neq 0$)

We show dynamic behavior with correlated noise η^t using computer simulations. In the case of $\delta > 0$, sample dependence appears and the network retrieves either memory or non-memory state even if retrieval from the same initial state. To examine functional roles of the correlated noise, we choose a sufficiently small independent noise, $\Delta = 0.2$. Figure 8 shows time evolutions of the overlap with correlated noise. The results are obtained from 20 samples using computer simulations ($N = 60,000$), where $\delta = 0.4$ or 0.5 and $r = 0.2$. Sample dependence occurs. When $\delta = 0.4$, the state is almost wrapped around the memory state, and when $\delta = 0.5$, it moves around the mixture state in several samples. Correlated noise can cause a transition from the memory to the mixture state stochastically.

Next, to verify that the state arrives at the mixture state, we consider a variation of the model that eliminates correlated noise after time $t = 50$. Figure 9 shows time evolution of the overlap, where $\delta = 0.5$ for $t \leq 50$ and $\delta = 0$ for $t > 50$. We find that the state wandering around the mixture state converges on the mixture state. Since the overlaps are distributed, we evaluate the marginal PDF of the overlap m_t^1 and compare the theoretical results with those obtained using computer simulations. Figure 10 shows the distribution of the overlap at time $t = 51$ and 60 . Abscissas denote the overlap m_t^1 , and ordinates denote the marginal PDF $p(m_t^1)$ on a logarithmic scale. Solid lines denote the marginal PDF obtained theoretically, and boxes denote histograms obtained using computer simulations. They show positive agreement. We find that the states are wandering around either the memory or mixture state.

4. conclusion

To analyze the functional roles of correlated noise, we investigated the associative memory models to which independent and correlated noises are introduced. In this paper, we analyzed two types of associative memory models: one with auto- and weak cross-correlation connections and one with hierarchically correlated patterns. In the former, we showed that correlated noise can switch from autoassociative to sequential associative memory. Switching memory systems is important for information processing. The most important point is that correlated noise is not random, but is added to all neurons mutually. In the latter, both the memory states and their mixture states are stable. Using only independent noise, the stochastic transition from the memory to the mixture state cannot be invoked, but sample dependence does appear and

the stochastic transition can be invoked using correlated noise.

In the case where sample dependence appears, the distribution of the overlaps needed to be analyzed to describe the macroscopic state. We, therefore, derived the macroscopic dynamic description as a recurrence relation form of probability density functions. The distributions obtained theoretically agree with those obtained using computer simulations. A transition between attractors cannot be invoked by thermal independent noise, but can be by synchronous spikes, indicated by Aoyagi and Aoki.^{6,7} This was demonstrated by our correlated external input, i.e., correlated noises. In this paper, we examined the cases when $p = 3$ for the former, and $p = 1$ and $k = 3$ for the latter. When $p \sim \mathcal{O}(1)$ and $k \sim \mathcal{O}(1)$, the behaviors for different values of p and k are qualitatively same as at present excepting stability of attractors.

Acknowledgment

This work was partially supported by a Grant-in-Aid for Scientific Research on Priority Areas No. 18020007 and No. 18079003, a Grant-in-Aid for Scientific Research (C) No. 16500093, and a Grant-in-Aid for Young Scientists (B) No. 16700210.

The computer simulation results were obtained using the PC cluster system at Yamaguchi University.

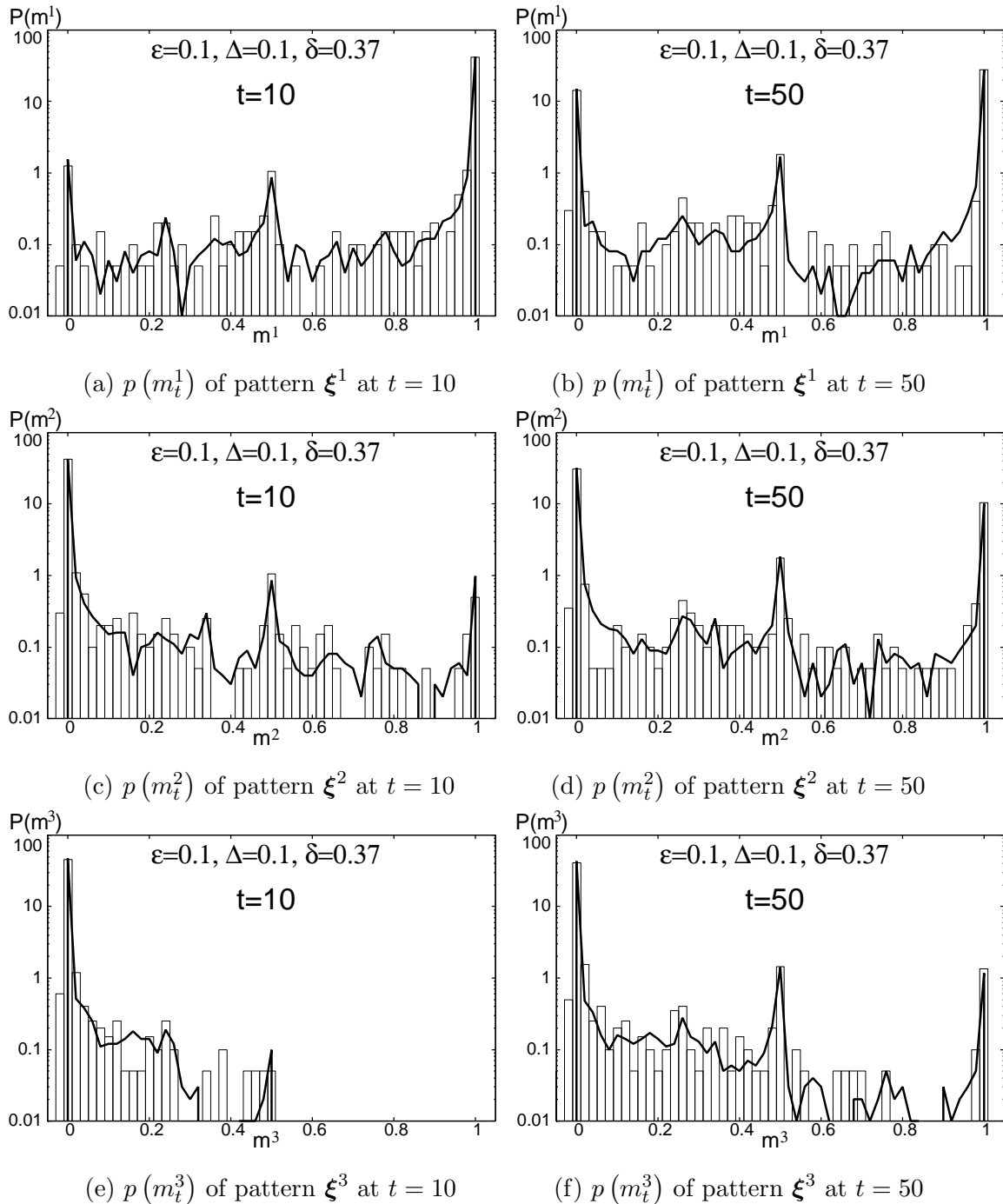


Fig. 5. Distribution of overlaps, m_t^1 , m_t^2 , and m_t^3 at time $t = 10, 50$, where $\varepsilon = 0.1, \Delta = 0.1$, and $\delta = 0.37$. Abscissas denote overlap and ordinates denote marginal PDF on a logarithmic scale. Boxes denote histograms obtained using computer simulations, and lines denote theoretical results. (a), (c), and (e) show results at $t = 10$, and (b), (d), and (f) show results at $t = 50$.

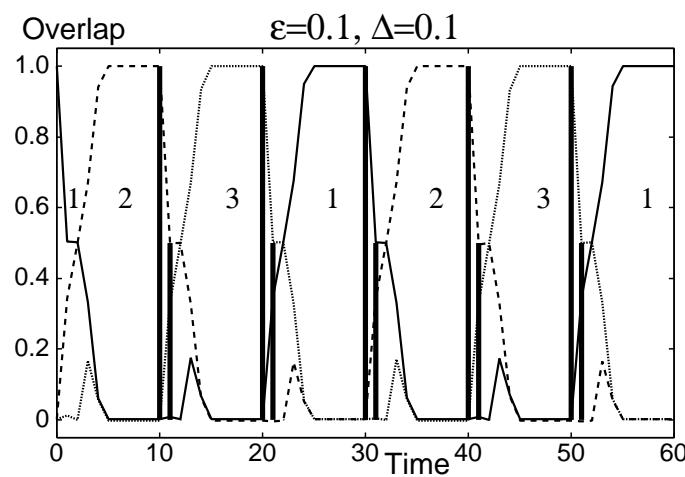


Fig. 6. Time evolutions of overlaps by particular common external input. Thick vertical lines denote the common external input.

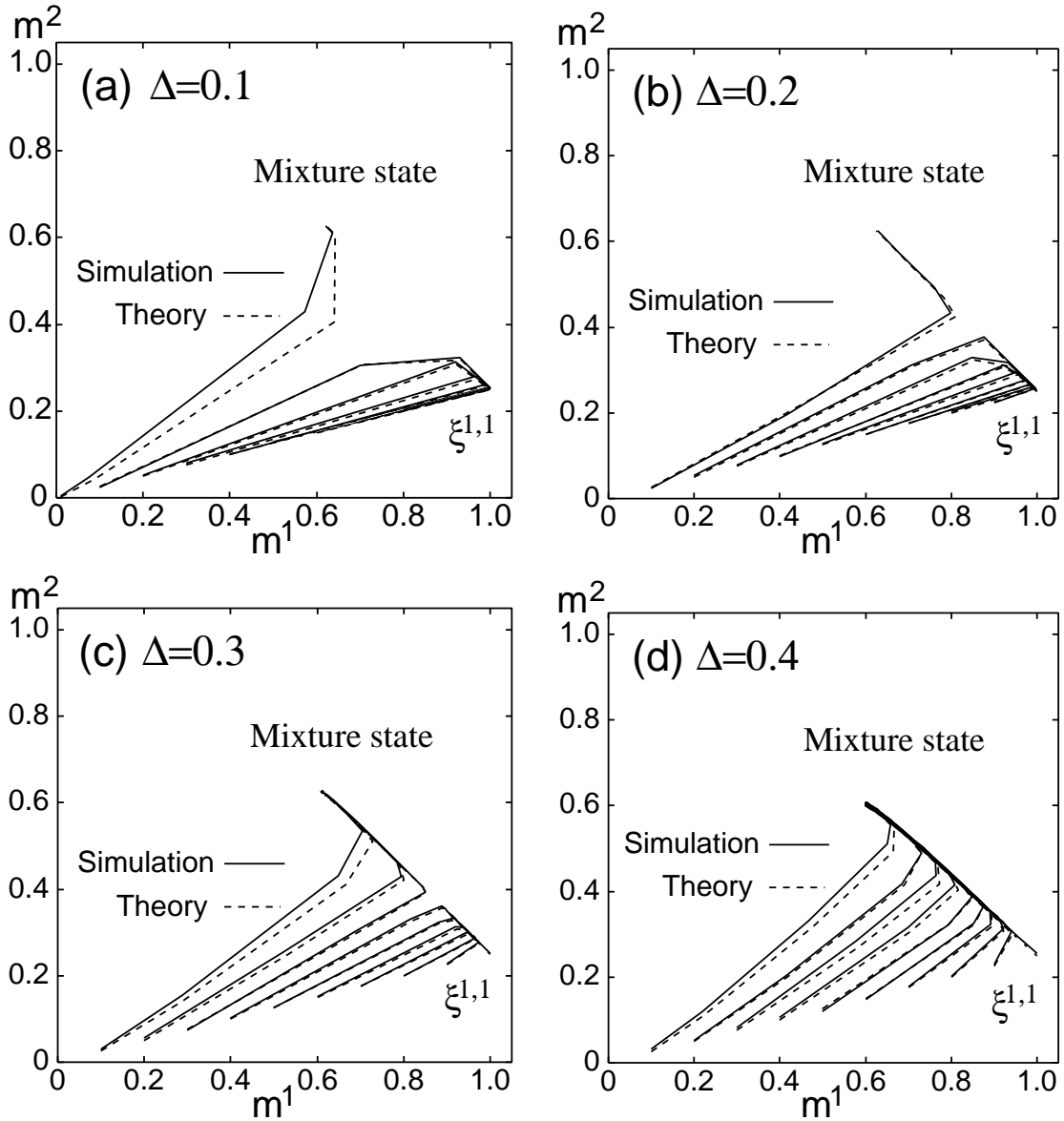


Fig. 7. Retrieval processes on (m_t^1, m_t^2) -plane, where $r = 0.5$ and (a) $\Delta = 0.1$, (b) $\Delta = 0.2$, (c) $\Delta = 0.3$, and (d) $\Delta = 0.4$.

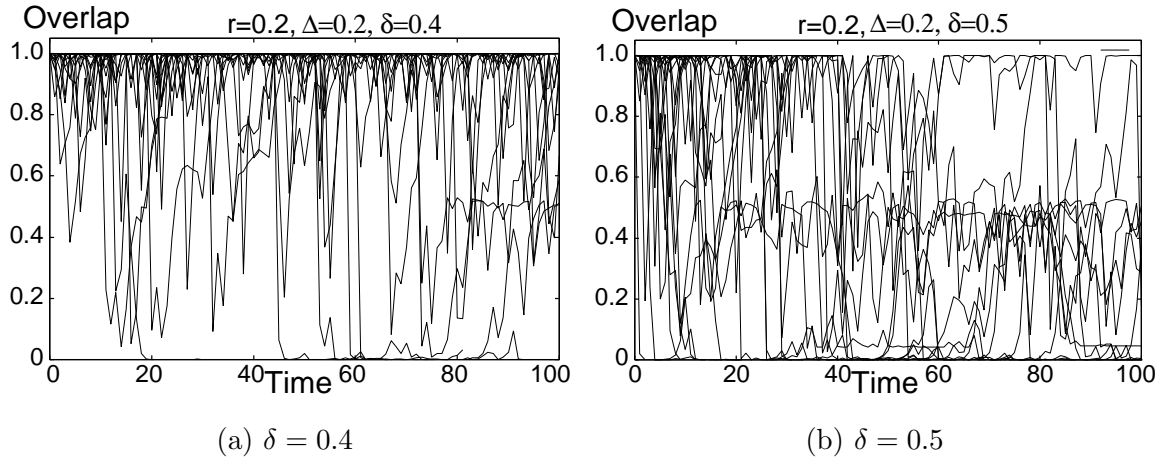


Fig. 8. Time evolution of overlap with correlated noise for (a) $\delta = 0.4$, and (b) $\delta = 0.5$, where $r = 0.2$ and $\Delta = 0.2$. The results are obtained from 20 samples using computer simulations.

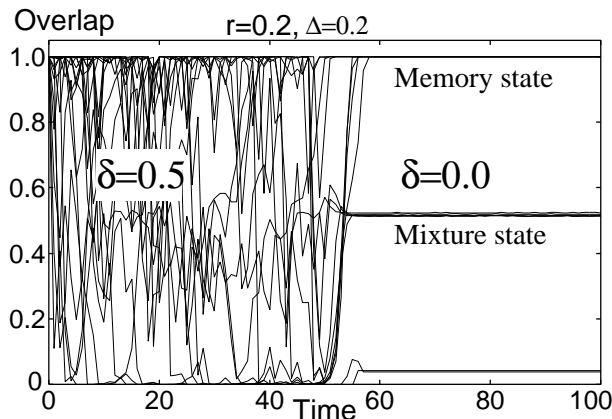


Fig. 9. Convergence of overlaps around the mixture state. Correlated noise is induced until $t < 50$.

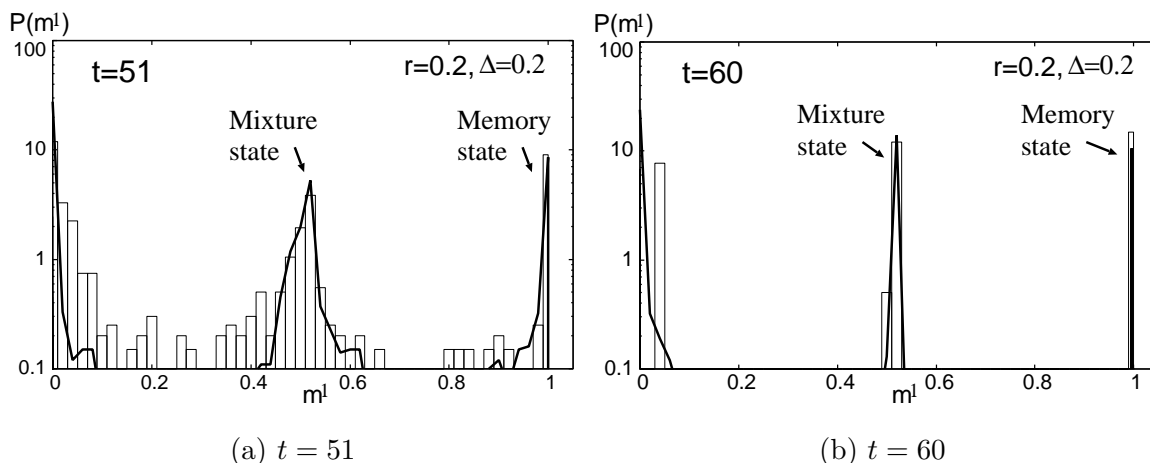
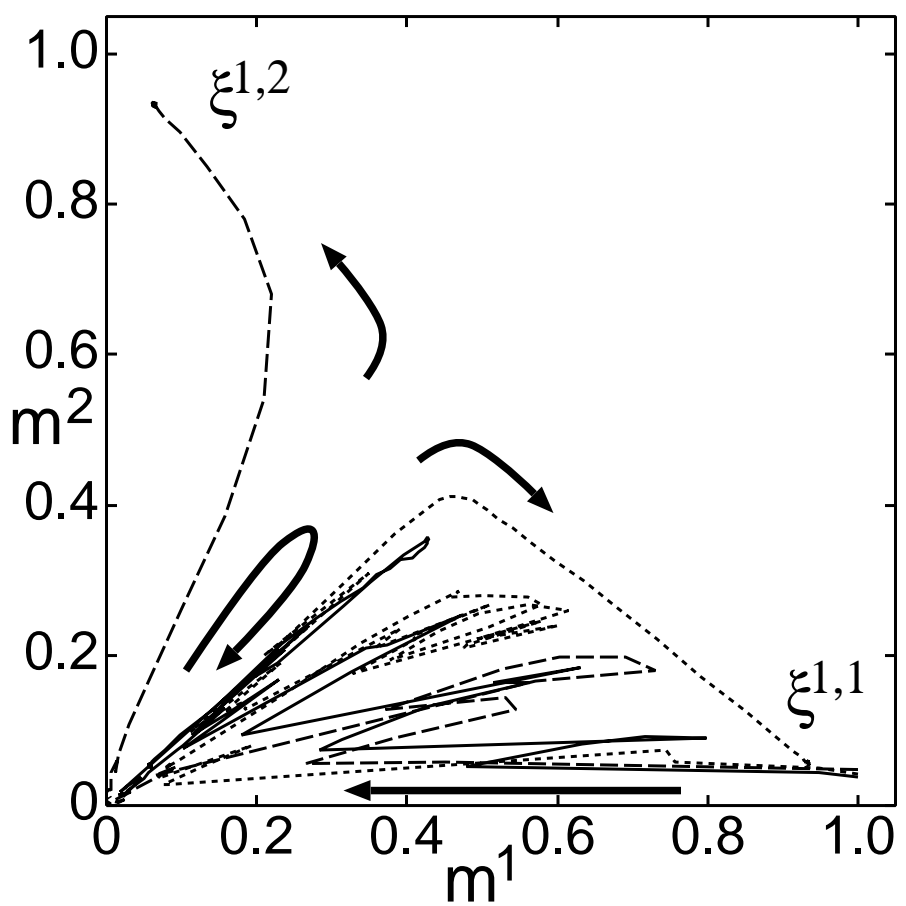
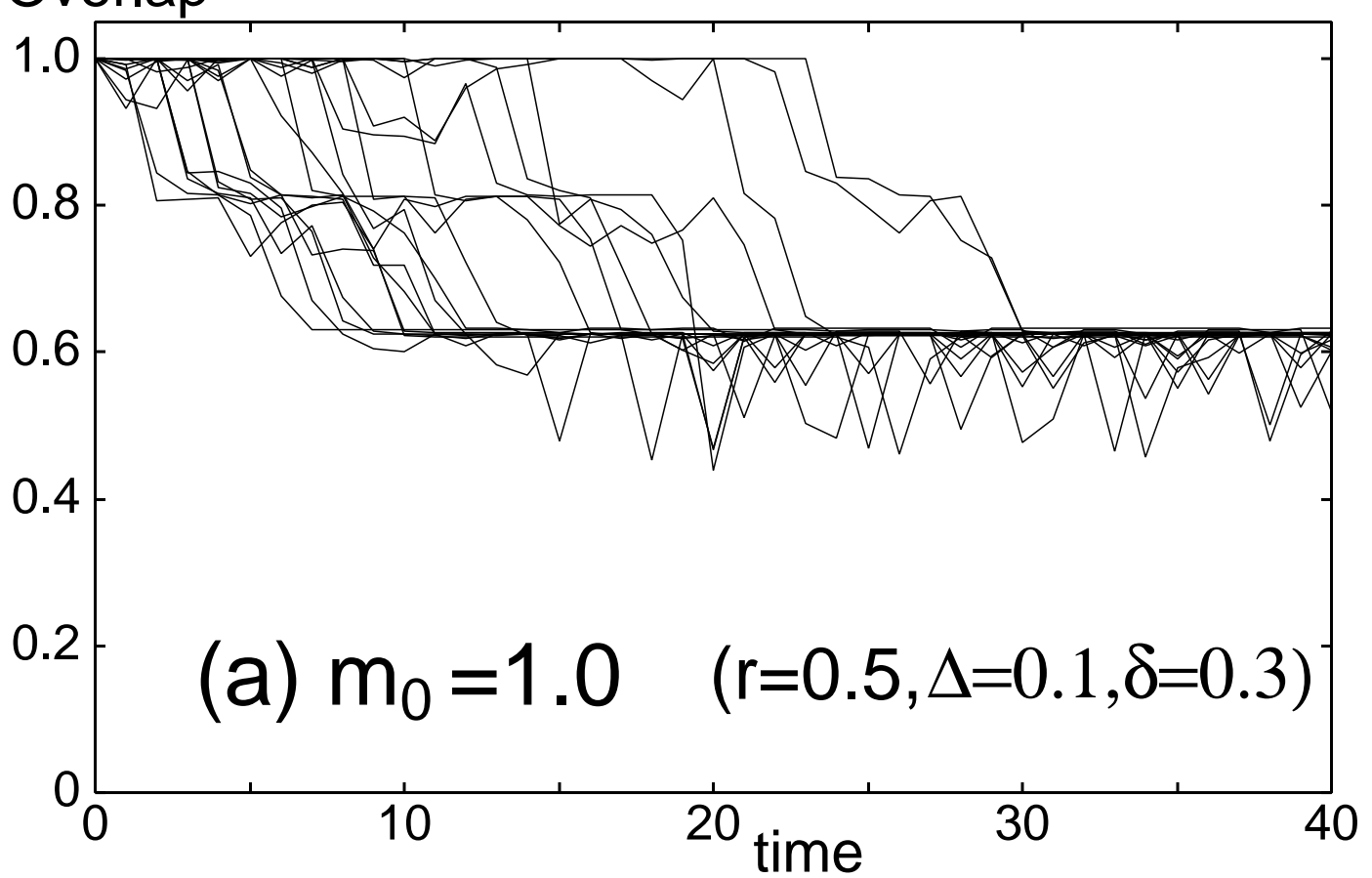


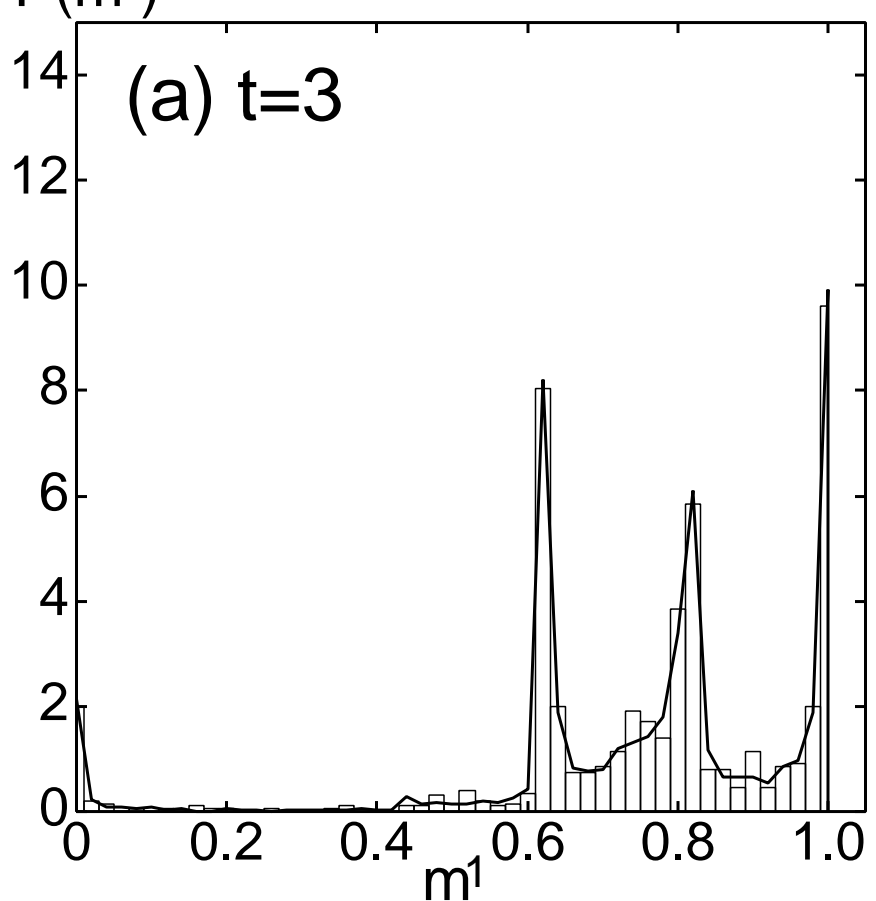
Fig. 10. Distribution of overlaps, $p(m_t^1)$, at (a) time $t = 51$, and (b) $t = 60$ in Fig. 9.

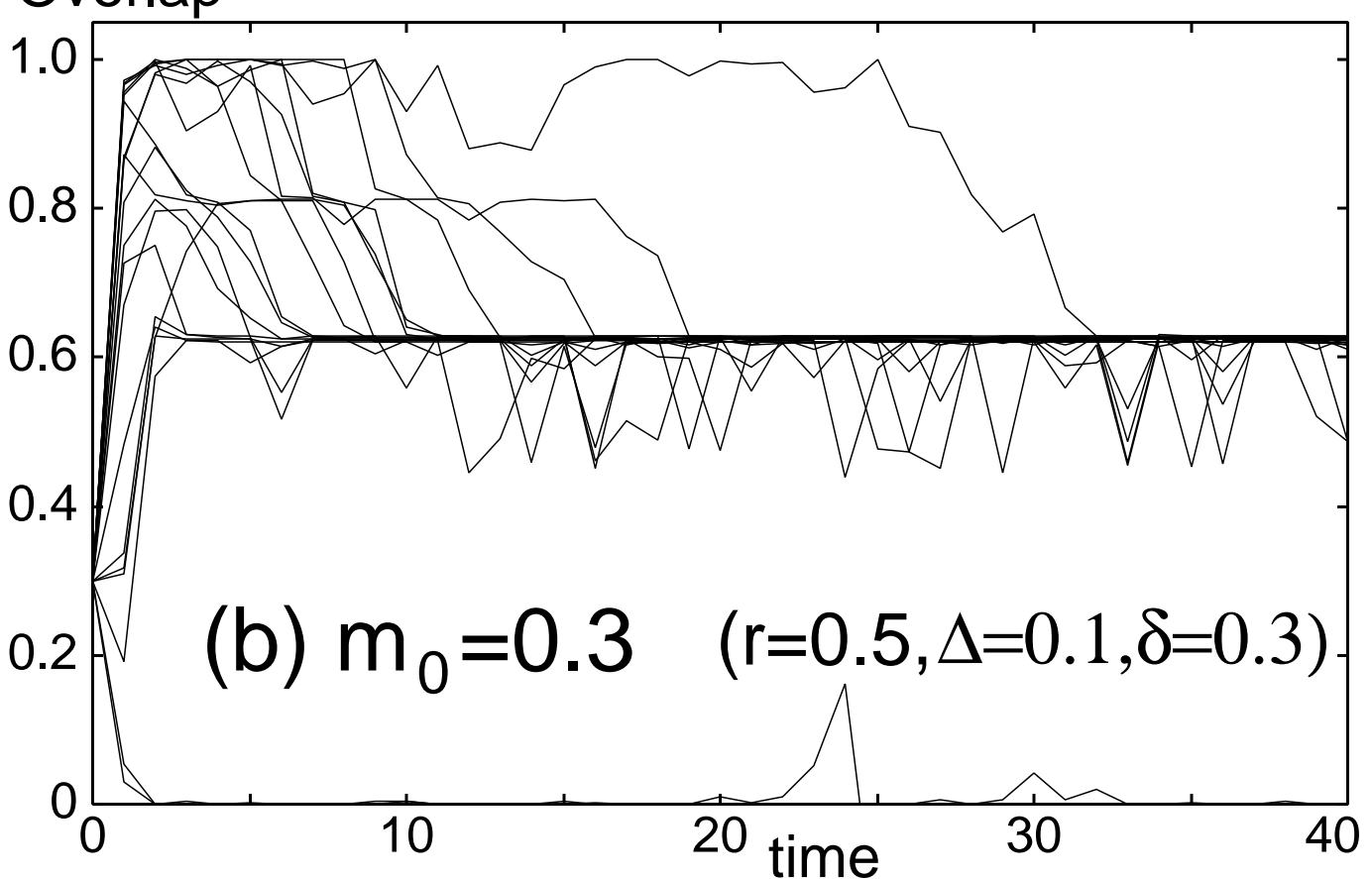
References

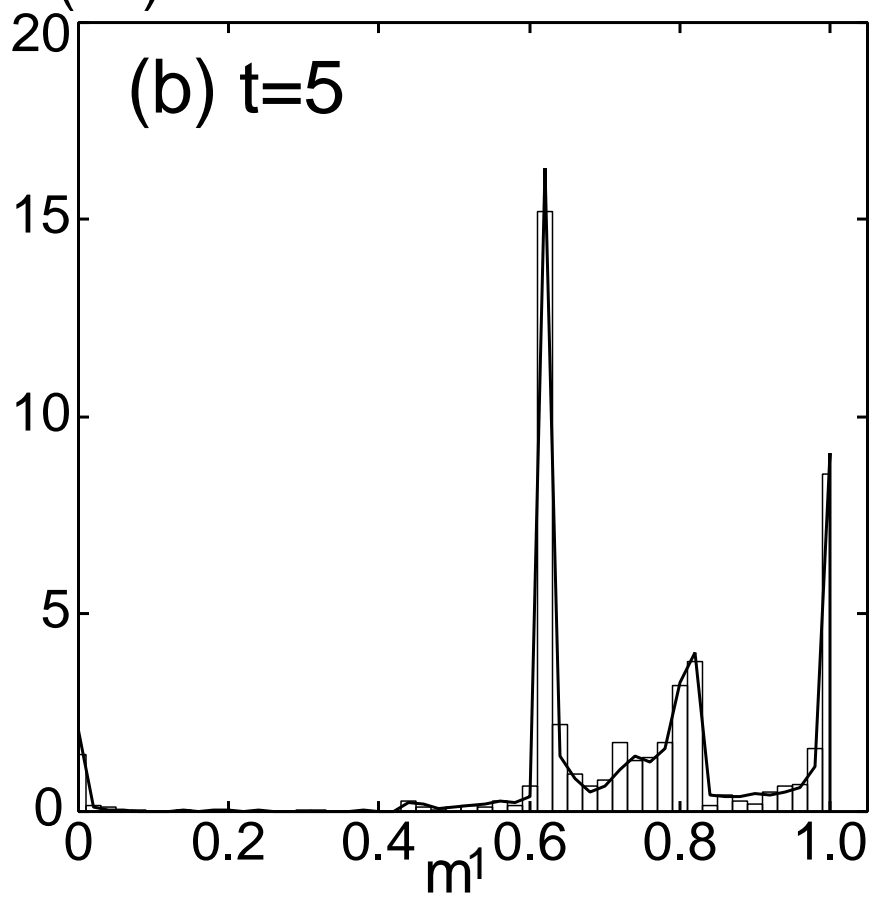
- 1) M. Abeles: Cambridge Univ. Press, Cambridge (1991).
- 2) M. Dlesmann, M.-O. Gewaltig, and A. Aertsen: *Nature* **402** (1999) 529.
- 3) H. Câteau and T. Fukai: *Neural Networks* **14** (2001) 675.
- 4) S. Amari, H. Nakahara, S. Wu, and Y. Sakai: *Neural Comp.* **15** (2003) 127.
- 5) M. Kawamura, M. Yamana, and M. Okada: *J. Phys. Soc. Jpn.* **74** (2005) 2961.
- 6) T. Aoyagi and T. Aoki: *Neurocomputing* **58–60** (2004) 259.
- 7) T. Aoki and T. Aoyagi: *Prog. Theor. Phys. Suppl.* **161** (2006) 152.
- 8) J. J. Hopfield: *Proc. Natl. Acad. Sci. USA* **79** (1982) 2554.
- 9) M. Okada: *Neural Networks* **8** (1995) 833.
- 10) S. Amari: *Proc. IEEE Conference on Neural Networks* **1** (1988) 633.
- 11) K. Kitano and T. Aoyagi: *J. Phys. A: Math. Gen.* **31** (1998) L613.
- 12) K. Katayama and T. Horiguchi: *J. Phys. Soc. Jpn.* **70** (2001) 1300.
- 13) M. Kawamura and M. Okada: *J. Phys. A: Math. Gen.* **35** (2002) 253.
- 14) M. Kawamura, M. Okada, and Y. Hirai: *IEEE Trans. Neural Networks* **10** (1999) 704.
- 15) S. Amari: *Biological Cybernetics* **26** (1977) 175.
- 16) N. Parga and M. A. Virasoro: *J. Physique* **47** (1986) 1857.
- 17) H. Gutfreund: *Phys. Rev. A* **37** (1988) 570.
- 18) H. Kakeya and T. Kindo: *Neural Networks* **9** (1996) 1095.
- 19) K. Toya, K. Fukushima, Y. Kabashima, and M. Okada: *J. Phys. A: Math. Gen.* **33** (2000) 2725.
- 20) D. J. Amit, H. Gutfreund, and H. Sompolinsky: *Phys. Rev. A* **32** (1985) 1007.
- 21) Y. Sakai: *BioSystems* **67** (2002) 221.
- 22) M. Yamana and M. Okada: *J. Phys. Soc. Jpn.* **74** (2005) 2260.
- 23) P. Peretto: *J. Physique* **49** (1988) 711.
- 24) M. Yoshioka and M. Shiino: *Phys. Rev. E* **55** (1997) 7401.
- 25) J. M. Cortes, J. J. Torres, J. Marro, P. L. Garrido, and H. J. Kappen: *Neural Comp.* **18** (2006) 614.
- 26) J. Hertz, A. Krogh, and R. G. Palmer: Perseus Books, chapter 2 (1991).

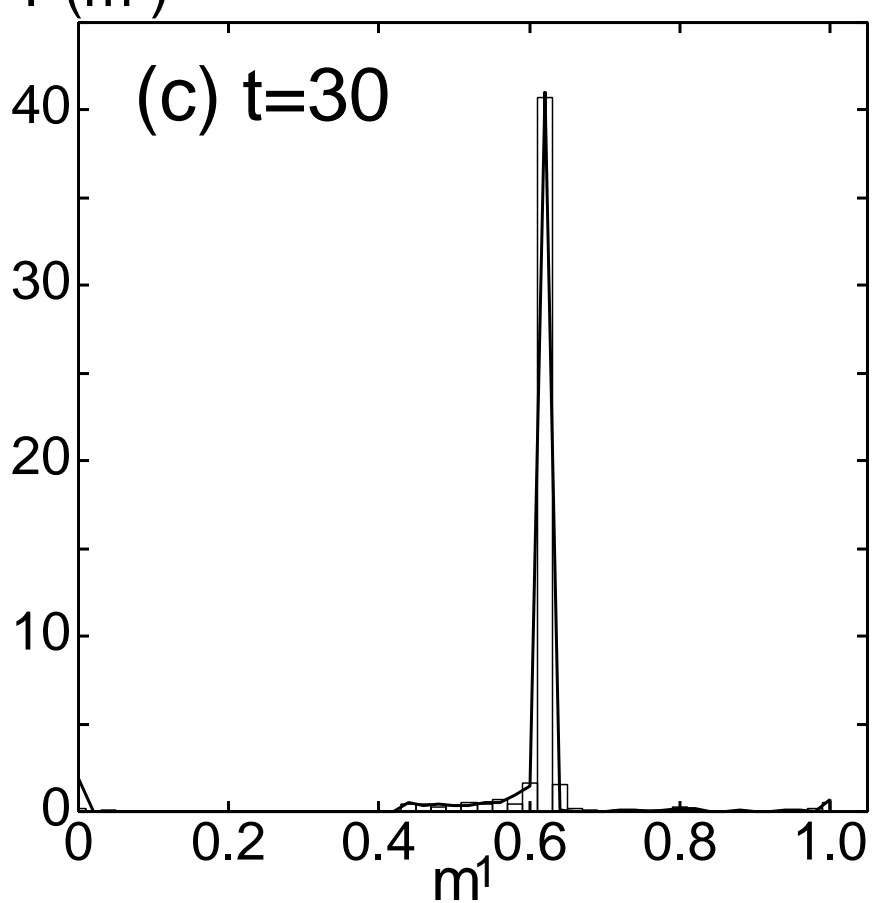


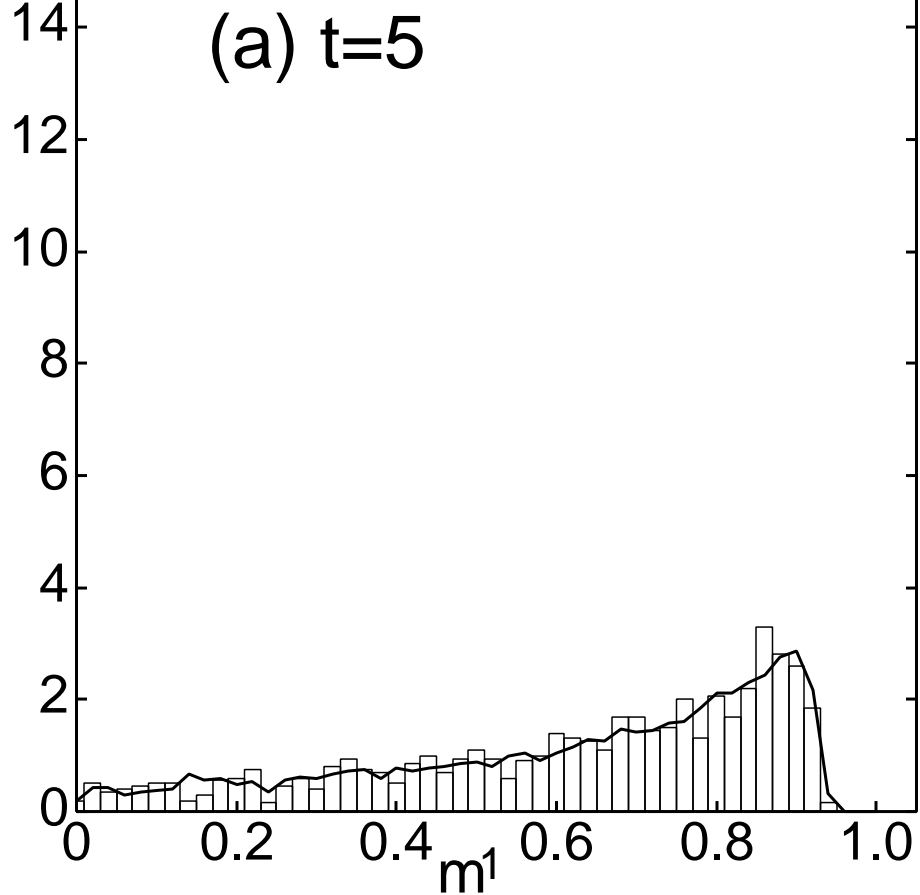


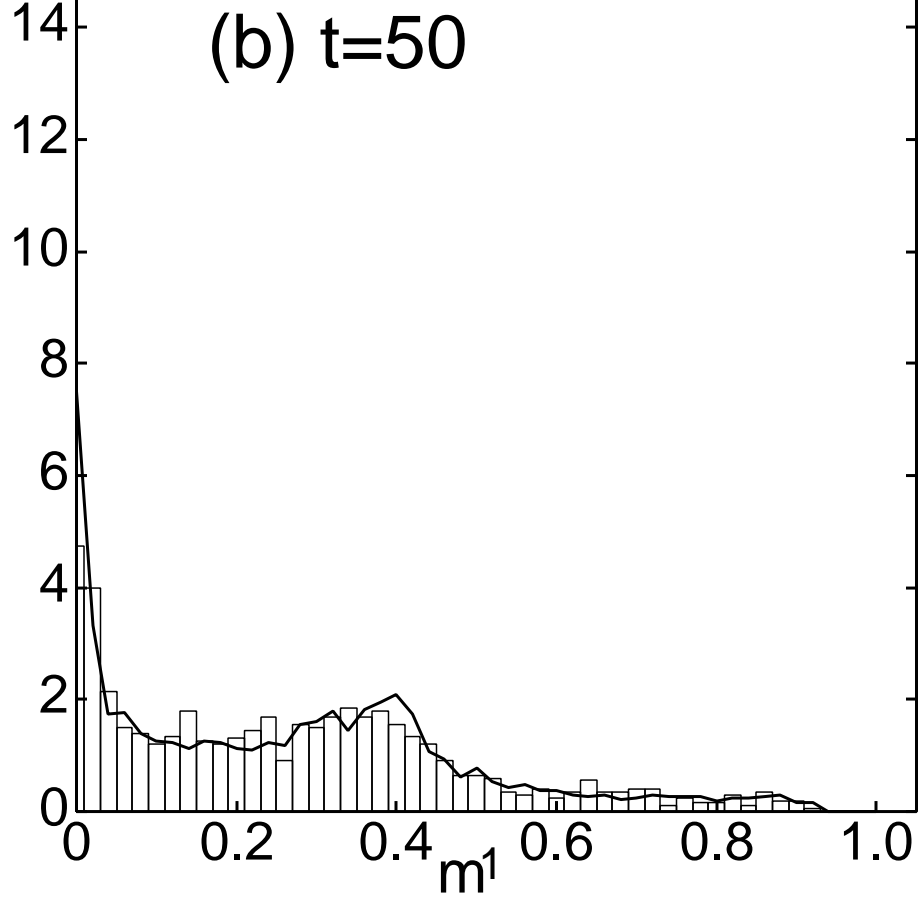




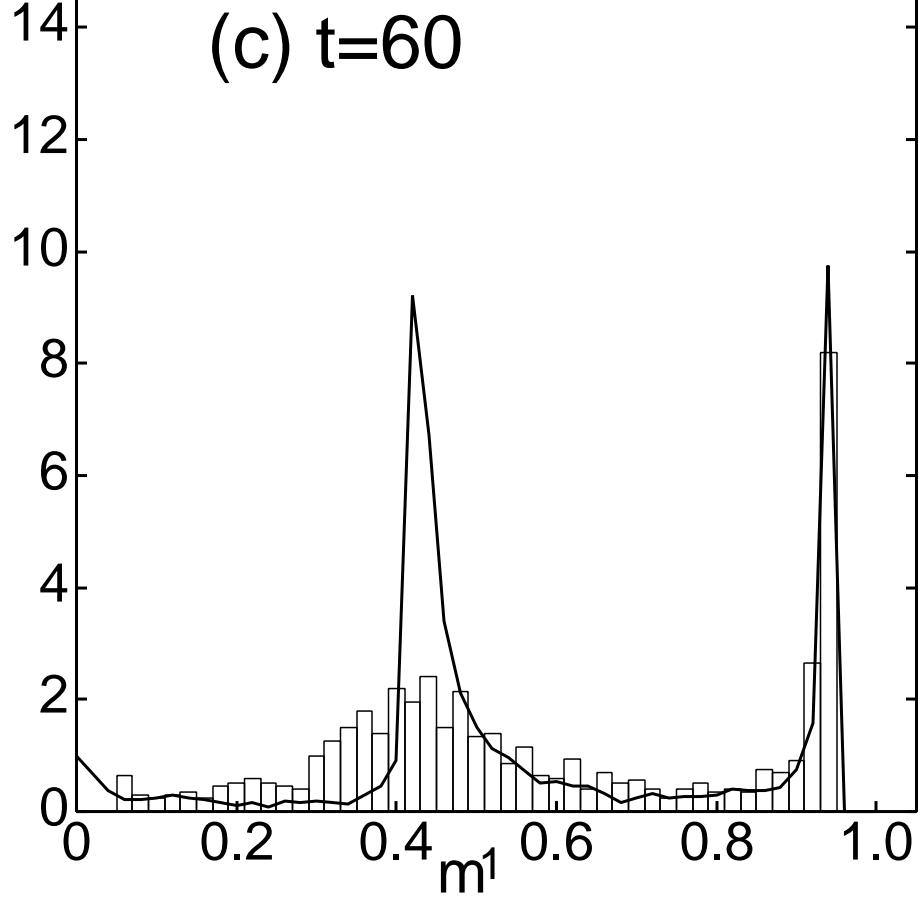








(c) $t=60$



(d) $t=80$

